ChemComm

Accepted Manuscript

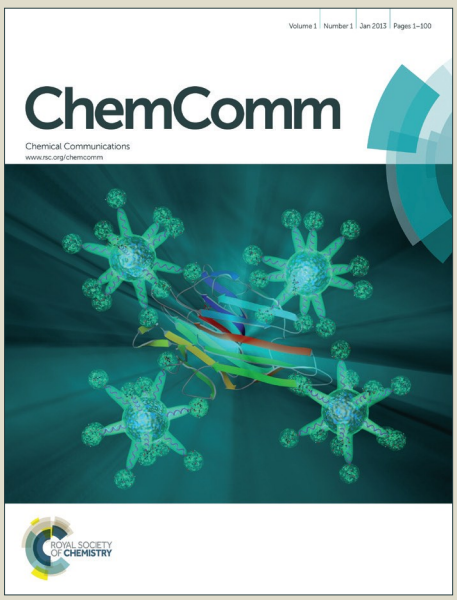

ROYAL SOCIETY OF CHEMISTRY

www.rsc.org/chemcomm

ChemComm

COMMUNICATION

Reactive Electrospinning of Degradable Poly(oligoethylene glycol methacrylate)-Based Nanofibrous Hydrogel Networks

· Received 00th January 20xx,
Accepted 00th January 20xx

DOI: 10.1039/x0xx00000x

www.rsc.org/

Fei Xu,[a] Heather Sheardown[a] and Todd Hoare[a]

A direct, all-aqueous electrospinning method for fabricating degradable nanofibrous hydrogel networks is reported in which hydrazide and aldehyde-functionalized poly(oligoethylene glycol methacrylate) (POEGMA) polymers are simultaneously electrospun and cross-linked. The resulting networks are spatially well-defined, mechanically stable (both dry and wet), and offer extremely fast swelling responses, suggesting potential utility as smart hydrogels and tunable tissue engineering matrices.

Hydrogels have attracted significant attention in biomedical applications due to their physicochemical and mechanical similarities to native extracellular matrix (ECM). While most hydrogels studied in this context have relatively homogeneous networks with pore sizes on the tens of nanometre scale, native ECM typically consists of gels constructed from a matrix of protein nanofibrils (primarily based on collagen and elastin). This fibrous structure has been demonstrated to play a key role in regulating how cells interact with the native ECM, influencing cell adhesion, spreading, and propagation.[1] However, replicating this nanofibrous hydrogel structure *in vitro,* particularly with synthetic polymers that offer the advantages of potentially reduced immunogenicity and increased tunability compared to natural polymers, has generally been challenging. Several examples of peptide-based nanofibrous hydrogels have been reported that exploit either the innate self-assembly of peptides or the directed self-assembly of typically hydrophobically modified peptides.[2–4] Research has also been done using synthetic small molecule amphiphiles[5,6] and synthetic block copolymers[7] as gelators to form nanofibrous hydrogels, although the physical nature of such self-assembly offers challenges for tuning hydrogel mechanics and stability to match specific application needs.

As an alternative to these physical self-assembly mechanisms for nanofiber formation, electrospinning represents a versatile technique for nanofiber preparation due to its low cost, high-throughput, and ready tunability based on changing process conditions (e.g. flow rates, voltages, collector distances)[8] While conventional electrospinning approaches generate solid nanofibers based on the rapid evaporation of volatile organic solvents between the spinner nozzle and the collector, organic solvent use limits the direct applicability of such methods in cell applications. Aqueous electrospinning of water-soluble polymers to form nanofibrous hydrogels is possible[9,10] but requires a method to stabilize the nanofibers (applied either during or after the spinning process) to form a hydrogel and prevent rapid dissolution upon re-exposure to water[11]. A variety of crosslinking methods have been reported, including chemical post-crosslinking by glutaraldehyde vapour[12,13] or by genipin[14] following nanofiber spinning, *in situ* crosslinking by glutaraldehyde using HCl as a catalyst[15] or maleic acid using vitriolic acid as catalyst[16], photocrosslinking by UV light during electrospinning[17–19] or physical crosslinking by heat treatment following electrospinning[20]. However, these methods may induce cytotoxicity, limiting their biomedical use. In addition, any post-treatment method mandates an additional processing step, and the resulting crosslink is either non-degradable (glutaraldehyde, photocrosslinking) or non-covalent. In this context, a single-step aqueous electrospinning method enabling production of a degradable, covalently crosslinked nanofibrous scaffold would be beneficial. The only such example is the work of Ji et al., who used Michael chemistry between thiolated hyaluronic acid and polyethylene glycol diacrylate to produce a nanofibrous hydrogel with promising cell migration and adhesion properties.[21,22] However, translation of this approach to synthetic polymers with non-degradable backbones would result in a non-degradable scaffold, again limiting biomedical applications.

Recently, we have reported injectable, covalently cross-linked poly(ethylene glycol) (PEG)-analogue hydrogels based on poly(oligoethylene glycol methacrylate) (POEGMA) formed via *in situ* gelation of low molecular weight precursor polymers functionalized with hydrazide and aldehyde functional groups. Poly (ethylene glycol) (PEG) is a hydrophilic, non-immunogenic, non-cytotoxic, and highly protein-repellent polymer[23–25], and PEG-based hydrogels are thus among the most widely used synthetic biomaterials for tissue engineering.[26,27] POEGMA offers many of the same properties as PEG (i.e. hydrophilicity, non-cytotoxicity, low protein adsorption)[28,29] but can be polymerized using standard free radical chemistries, enabling

[a] Department of Chemical Engineering, McMaster University, 1280 Main St. W., Hamilton, Ontario, Canada L8S 4L7; E-mail: hoaretr@mcmaster.ca

Electronic Supplementary Information (ESI) available: complete experimental details, analysis of precursor polymers, videos of swelling and mechanical testing experiments]. See DOI: 10.1039/x0xx00000x

facile functionalization of POEGMA-based networks to tune the mechanical and biological properties as desired. With our particular approach, covalent crosslinking of hydrazide and aldehyde-functionalized precursor polymers via the formation of hydrolytically and enzymatically-degradable hydrazone bonds offers additional advantages. Hydrazone bond formation facilitates rapid gelation and tunable degradation according to the structure and reactive functional group density of the POEGMA precursor polymer. The absence of any small molecule crosslinkers or need for heat/UV light to facilitate gelation promotes higher cytocompatibility relative to other possible strategies, **with cell viability demonstrated in both 2D and 3D culture**.[30] The ease of functionalizing POEGMA backbones by copolymerization enables conjugation of controlled densities of cell adhesion-modifying peptides or other ligands to engineer the cell-hydrogel interface.[31] Furthermore, depending on the length of the oligo(ethylene glycol) side chain in the OEGMA monomer used, the hydrogel can be engineered to exhibit "smart" thermoresponsive properties that can further be applied to (for example) dynamically tune cell-gel interactions[30] or facilitate environmentally-responsive drug delivery.[32] Of note, given the typically sluggish swelling kinetics of thermoresponsive bulk hydrogels, the formation of nanofibrous (macroporous) hydrogels based on POEGMA in a single step without requiring any pore-forming additives offers potential to enhance the rate and reversibility of thermal swelling/deswelling transitions[33] while maximizing the network cytocompatibility.

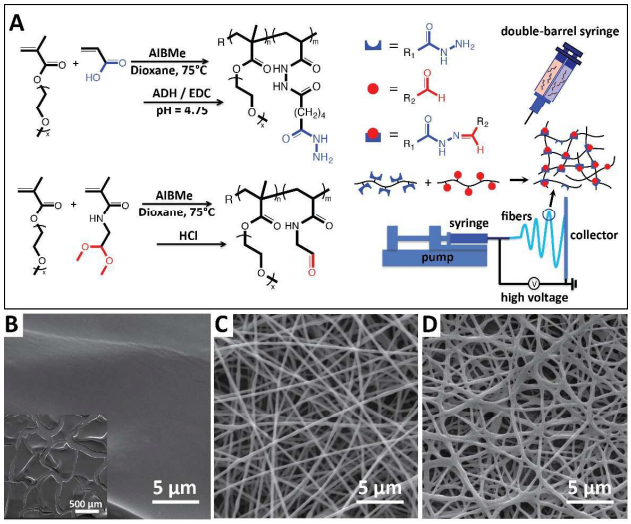

Figure 1: Reactive electrospinning of degradable POEGMA hydrogel nanofibers: (A) scheme showing polymer precursor chemistry and electrospinning strategy; (B-D) electrospun POH/POA only (B), PEO only (C), and POH/POA+PEO (D).

To leverage these favorable properties of POEGMA and nanofibrous hydrogels, we have developed a reactive electrospinning process to directly fabricate degradable nanofibrous POEGMA hydrogels in a single step (Fig. 1A). POEGMA precursor polymers with molecular weights on the order ~30 kDa (to facilitate kidney clearance following gel degradation via hydrolysis, Table S1) were functionalized with 30 mol% hydrazide groups (POH, via carbodiimide-mediated adipic acid dihydrazide conjugation to an acrylic acid-functionalized POEGMA polymer) and aldehyde groups (POA, via copolymerization of OEGMA with a diacetal-containing monomer followed by acid-catalyzed cleavage of the diacetal to an aldehyde) following reported protocols.[31] Each polymer was then dissolved at 15% w/v in deionized water and loaded into separate barrels of a double barrel syringe attached to a static mixer with a blunt 18G needle at its outlet. This syringe was mounted on a syringe pump and connected to an electrospinning platform. The bulk gelation time of the POEGMA prepolymers used was ~45 minutes; a flow rate of 8 µL/min was subsequently selected to match the residence time of the polymer in the mixing channel to the gelation rate and thus ensure both spinnability (i.e. minimal increases in viscosity prior to jetting) and stable nanofiber formation on the collector. The increase in polymer concentration during the spinning step assists with enabling both these competing requirements, as a solution just below its gel point can be ejected but then rapidly stabilized via covalent network formation as it is concentrated upon water evaporation. A voltage of 8.5 kV was applied to the conductive needle, with either aluminium foil (for films) or an aluminium disk (for bulk scaffolds) used as a collector (Fig. S1). Using POEGMA alone (POA/POH, Fig. 1B) resulted in electrospray at all process conditions tested; we anticipate this observation is a result of both the high hygroscopicity and low entanglement potential of the low molecular weight and highly side chain-branched POEGMA polymer, properties previously shown to inhibit polymer spinnability[34–36]. In response, a small concentration of high molecular weight poly(ethylene oxide) (PEO, M_v = 600×10^3 g/mol, 5% w/v dissolved in deionized water, 1:3 weight ratio PEO:POEGMA) was introduced as an electrospinning aid. The high molecular weight and chain flexibility of PEO enables its electrospinning from aqueous solutions to form well-defined nanofibers[9,37,38] (Fig. 1C); furthermore, its chemical similarity to POEGMA facilitates mixing without phase separation during electrospinning or drying. PEO nanofibers alone exhibited a diameter of 287 ± 80 nm (Fig. 1C); when PEO was mixed with hydrazide and aldehyde POEGMA precursors (POH/POA+PEO, Fig. 1D), a single nanofibrous network with an average fiber diameter of 341 ± 82 nm was achieved, with no evidence of electrosprayed nanoparticle generation visually or microscopically (Fig. 1D).

Upon exposure to phosphate buffered saline (PBS), PEO-only nanofibers dissolved fully within one minute; in contrast, the POH/POA+PEO electrospun matrix quickly hydrated and swelled but remained present as a gel matrix (see video in Supplementary Information). The disappearance of the characteristic PEO phase transition peak at ~65-70°C via differential scanning calorimetry following soaking of the gel in deionized water overnight indicates that PEO electrospinning aid can be effectively removed from the matrix **while maintaining the nanofibrous structure** (Figs. S2 and S3). Light microscopy analysis of the swollen fiber mat confirmed the presence of a fibrous structure (Fig. 2A) relative to the bulk hydrogel prepared from the same starting components (Fig. 2B); furthermore, when half the POA/POH+PEO scaffold was dipped in water, scanning electron microscopy imaging of the subsequently lyophilized sample indicated a clear increase in nanofiber diameter between the swollen (wetted) matrix (1.33 ± 0.20 µm) and the still-dry nanofibers not exposed to water (0.34 ± 0.08 µm), although a textured nanofibrous structure was maintained in the swollen state (Fig. 2C). Confocal microscopy of electrospun POH/POA+PEO nanofibers using

POH labelled with fluorescein isothiocyanate (green, 488 nm) and POA labelled with rhodamine (red, 543 nm) demonstrated that both fluorescent signals were uniformly present throughout the nanofiber mat (Fig. 2E), confirming the co-localization of reactive precursor polymers as required for gelation. The presence of POEGMA in the nanofibers following soaking was also confirmed by ATR-FTIR via the presence of a C=O ester stretch at ~1700 cm^{-1} corresponding to the attachment point between the methacrylate backbone and the oligo(ethylene glycol) side chains (Fig. 2D). Thus, the nanofibers following soaking appear to consist primarily of cross-linked POEGMA and behave as a hydrogel matrix.

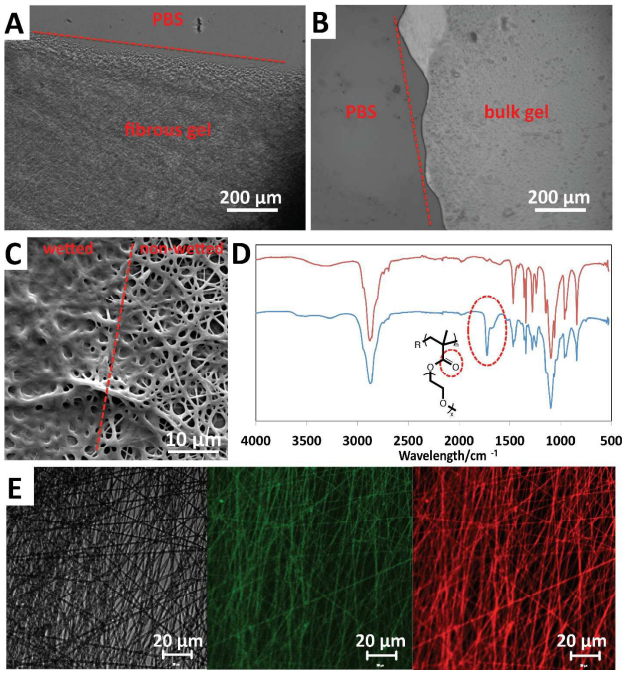

Figure 2: Confirmation of hydrogel structure of POH/POA+PEO nanofibers: (A, B) light microscopy images of electrospun nanofibers (A) relative to a bulk hydrogel of the same chemical composition (B) in 10 mM PBS; (C) scanning electron microscopy image of nanofibers dipped halfway in water; (D) ATR-FTIR analysis of PEO-only (red) and POH/POA+PEO (blue) nanofibers; (E) co-localization of POH-fluorescein (488 nm excitation, green) and POA-rhodamine (543 nm excitation, red) throughout nanofiber structure (visible light, grey).

The swelling and degradation properties of the POH/POA+PEO nanofibers were subsequently analysed via gravimetric analysis at 37 °C in 10 mM PBS, mimicking physiological conditions. Swelling of the dry nanofibrous hydrogel mat occurred rapidly, with the maximum water content of ~91 % achieved in less than one minute (Fig. 3A) followed by minimal deswelling over the next 50 hours (Fig. S4, likely attributable to diffusion of the PEO out of the matrix and the corresponding loss of osmotic driving force for gel swelling). In comparison, a (pre-dried) bulk hydrogel of the same POH/POA composition required ~2 hours to achieve equilibrium swelling and reached only ~73% water content (Figs. 3A and S4). This rapid and higher-magnitude swelling facilitated by the nanofibrous network structure is of potential interest in barrier applications (e.g. following abdominal surgeries) given that the gel could be stored dry in a mat but quickly re-hydrated to prevent tissue adhesions. In addition, while the transition temperature of the current POEGMA hydrogels is > 90 °C such that it is not functionally thermoresponsive in water[30], we expect precursor polymers with lower LCST values would also exhibit faster and higher magnitude swelling/deswelling responses for the same reason.

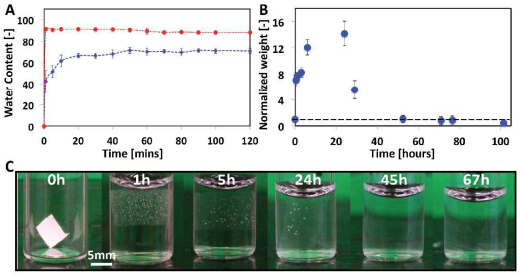

Figure 3: Swelling and degradation of POH/POA+PEO nanofibers: (A) swelling of nanofiber mat (red) relative to a bulk hydrogel (blue) of the same composition (PBS, 37°C); (B, C) gravimetric (B) and visual (C) degradation (normalized to initial dry hydrogel mass) of nanofibers (1M HCl, 37°C).

Incubation of the same dry electrospun network in 1M HCl (to acid-catalyze degradation of hydrazone cross-links under accelerated conditions) results in initial swelling of the gel over the course of ~24 hours (corresponding to a combination of re-hydration plus swelling due to degradation of the hydrazone cross-links) followed by complete dissolution of the network within ~100 hours (Figs. 3B and 3C). **SEM indicates a loss of fibrous morphology over this same time period (Fig. S5), consistent with degradation.** Similar experiments in PBS indicated complete dissolution of the network over 8-10 weeks. Based on our previous work[31], the degradation kinetics could be further adjusted if desired by changing the number of reactive functional groups on POH and/or POA or the concentration of POEGMA used to prepare the nanofibers.

The resulting nanofiber hydrogels are mechanically strong and coherent in both the wet and dry states, at least relative to other hydrogel-based systems, and could be physically handled with ease. Tensile cycling of the dry POH/POA+PEO scaffold was performed using a MicroSquisher (CellScale Biomaterials Testing) by mounting the scaffold via 5 puncture pins and performing cyclic 20% stretching experiments in tensile mode. While significant plastic deformation was observed over the first 6 cycles (reducing the peak force observed by roughly one half), the dry matrix remained intact after 80 cycles, with full elastic recovery of the matrix observed each cycle following the initial deformation period (Figs. 4A and S6a). **Tensile testing of the 10 mM PBS-swollen POH/POA+PEO gel (10% elongation) over >300 cycles yielded a tensile modulus of ~0.3 kPa (Table S2, Fig. S7), while c**ompression testing (50% compression) yielded an elastic modulus of 2.1 kPa maintained over at least 40 cycles with minimal hysteresis (Figs. 4B and S4b). Note that a bulk hydrogel with the same overall composition has a compressive modulus of 4.8 kPa under the same testing conditions (Table S3); furthermore, the compressive modulus of the bulk hydrogel is constant as a function of the compressive strain while nanofibrous hydrogels show higher moduli at higher % compressions as the space between the nanofibers is compressed (Table S3). Thus, nanofibrous gels have mechanics

relevant for use in both the wet and dry states.

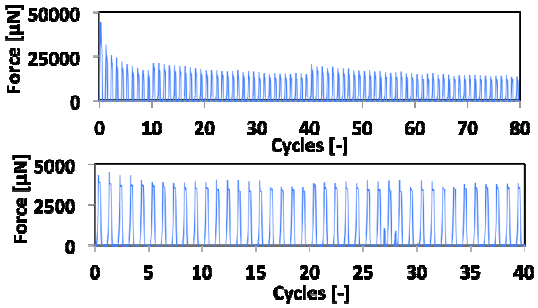

Figure 4: Mechanical properties of POH/POA+PEO nanofibers: (A) tensile cycling of dry nanofiber mat (80 cycles, 20% elongation/cycle); (B) compressive cycling of swollen nanofiber network (PBS, 40 cycles, 50% compression/cycle).

Finally, direct encapsulation of alkaline phosphatase (ALP) or β-galactosidase (β-gal) by mixing the enzyme in the POH solution prior to electrospinning indicated that the scaffolds can maintain >80% (ALP) or ~60% (β-gal) activity in the released enzyme fraction over multiple days (Fig. S8). This activity retention is significantly higher than achieved with conventional electrospinning[39] and is thus suggestive of the relative inertness of this method to biomolecules.

In summary, a single-step, all-aqueous reactive electrospinning process is demonstrated to successfully produce synthetic degradable nanofibrous hydrogels based on POEGMA without the need for solvents or external cross-linkers. POEGMA/PEO electrospun nanofibers swell rapidly (reaching equilibrium within 1 min., compared to ~2 hrs for a bulk hydrogel), degrade over the period of ~2 days in acidic conditions and ~8 weeks in physiological buffer (with the potential to tune this degradation rate by polymer modification), exhibit relevant mechanical properties for biomedical use, and can maintain high enzyme activity. We anticipate possible applications of these nanofibrous scaffolds in both the dry state (wound dressings, barrier materials) and the wet state (tissue engineering matrices, drug delivery).

Notes and references

‡ Funding from the Natural Sciences and Engineering Research Council of Canada and the NSERC CREATE-IDEM (Integrated Development of Extracellular Matrices) training program is gratefully acknowledged. José Moran-Mirabal is thanked for use of his electrospinning equipment and helpful advice.

1 M. M. Stevens, J. H. George, *Science*, 2005, **310**, 1135–1138.
2 L. E. R. O'Leary, J. A. Fallas, E. L. Bakota, M. K. Kang, J. D. Hartgerink, *Nat. Chem.*, 2011, 3, 821–828.
3 J. Luo, Y. W. Tong, *ACS Nano*, 2011, **5**, 7739–7747.
4 E. C. Wu, S. Zhang, C. A. E. Hauser, *Adv. Funct. Mater.*, 2012, **22**, 456–468.
5 P. K. Vemula, J. E. Kohler, A. Blass, M. Williams, C. Xu, L. Chen, S. R. Jadhav, G. John, D. I. Soybel, J. M. Karp, *Sci. Rep.*, 2014, **4**, 4466–4469.
6 V. Jayawarna, M. Ali, T. A. Jowitt, A. F. Miller, A. Saiani, J. E. Gough, R. V. Ulijn, *Adv. Mater.*, 2006, **18**, 611–614.
7 A. Blanazs, R. Verber, O. O. Mykhaylyk, A. J. Ryan, J. Z. Heath, C. W. I. Douglas, S. P. Armes, *J. Am. Chem. Soc.*, 2012, **134**, 9741–9748.
8 A. Greiner, J. H. Wendorff, *Angew. Chemie - Int. Ed.*, 2007, **46**, 5670–5703.
9 J. Doshi, D. H. Reneker, *Conf. Rec. 1993 IEEE Ind. Appl. Conf. Twenty-Eighth IAS Annu. Meet.*, 1993, **35**, 151–160.
10 Y. Yang, Z. Jia, Q. Li, Z. Guan, *IEEE Trans. Dielectr. Electr. Insul.*, 2006, **13**, 580–584.
11 L. Yao, T. W. Haas, A. Guiseppi-Elie, G. L. Bowlin, D. G. Simpson, G. E. Wnek, *Chem. Mater.*, 2003, **15**, 1860–1864.
12 J. D. Schiffman, C. L. Schauer, *Biomacromolecules*, 2007, **8**, 594–601.
13 K. S. Rho, L. Jeong, G. Lee, B. M. Seo, Y. J. Park, S. D. Hong, S. Roh, J. J. Cho, W. H. Park, B.-M. Min, *Biomaterials*, 2006, **27**, 1452–1461.
14 M. E. Frohbergh, A. Katsman, G. P. Botta, P. Lazarovici, C. L. Schauer, U. G. K. Wegst, P. I. Lelkes, *Biomaterials*, 2012, **33**, 9167–9178.
15 C. Tang, C. D. Saquing, J. R. Harding, S. A. Khan, *Macromolecules*, 2010, **43**, 630–637.
16 X. H. Qin, S. Y. Wang, *J. Appl. Polym. Sci.*, 2008, **109**, 951–956.
17 S. H. Kim, S. H. Kim, S. Nair, E. Moore, *Macromolecules*, 2005, **38**, 3719–3723.
18 Y. Wang, C. Cheng, Y. Ye, Y. Yen, F. Chang, 2012, 8–11.
19 E. Baştürk, B. Oktay, M. V. Kahraman, *J. Polym. Res.*, 2015, **22**, 133.
20 S. J. Lee, S. G. Lee, H. Kim and W. S. Lyoo, *J. Appl. Polym. Sci.*, 2007, **106**, 3430–3434.
21 Y. Ji, K. Ghosh, B. Li, J. C. Sokolov, R. A. F. Clark and M. H. Rafailovich, *Macromol. Biosci.*, 2006, **6**, 811–817.
22 Y. Ji, K. Ghosh, X. Z. Shu, B. Li, J. C. Sokolov, G. D. Prestwich, R.A.F. Clark, M. H. Rafailovich, *Biomaterials*, 2006, **27**, 3782-3792.
23 M. E. Price, R. M. Cornelius, J. L. Brash, *Biochim. Biophys. Acta - Biomembr.*, 2001, **1512**, 191–205.
24 W. Feng, S. Zhu, K. Ishihara, J. L. Brash, *Biointerphases*, 2006, **1**, 50–60.
25 S. Alibeik, S. Zhu, J. L. Brash, *Colloids Surfaces B Biointerfaces*, 2010, **81**, 389–396.
26 N. A. Peppas, J. Z. Hilt, A. Khademhosseini, R. Langer, *Adv. Mater.*, 2006, **18**, 1345–1360.
27 C. C. Lin, K. S. Anseth, *Pharm. Res.*, 2009, **26**, 631–643.
28 J.-F. Lutz, *J. Polym. Sci. A.*, 2008, **46**, 3459–3470.
29 J.-F. Lutz, A. Hoth, *Macromolecules*, 2006, **39**, 893–896.
30 N. M. B. Smeets, E. Bakaic, M. Patenaude, T. Hoare, *Acta Biomater.*, 2014, **10**, 4143–4155.
31 N. M. B. Smeets, E. Bakaic, M. Patenaude, T. Hoare, *Chem. Commun.*, 2014, **50**, 3306–3309.
32 E. Bakaic, N. M. B. Smeets, H. Dorrington, T. Hoare, *RSC Adv.*, 2015, **5**, 33364–33376.
33 W. Cai, R. B. Gupta, *J. Appl. Polym. Sci.*, 2002, **83**, 169–178.
34 S. Ramakrishna, K. Fujihara, W.-E. Teo, T.-C. Lim, Z. Ma, *An Introduction to Electrospinning and Nanofibers*, 2005.
35 S. L. Shenoy, W. D. Bates, H. L. Frisch, G. E. Wnek, *Polymer*, 2005, **46**, 3372–3384.
36 P. Gupta, C. Elkins, T. E. Long, G. L. Wilkes, *Polymer*, 2005, **46**, 4799–4810.
37 H. Fong, I. Chun and D. H. Reneker, *Polymer*, 1999, **40**, 4585–4592.
38 R. Jaeger, M. M. Bergshoef, C. M. I. Batlle, H. Schönherr, G. Julius Vancso, *Macromol. Symp.*, 1998, **127**, 141–150.
39 Y. Dror, J. Khun, R. Avrahami, E. Zussman, *Macromolecules*, 2008, **41**, 4187-4192.